Archives
of Materials Science
and Engineering

Volume 29
Issue 2
February 2008
Pages 89-92

International Scientific Journal
published monthly by the
World Academy of Materials
and Manufacturing Engineering

Influence of initial heat treatment on the fatigue life of austenitic Fe–Ni alloy

K.J. Ducki *, M. Cieśla
Materials Science Department, Silesian University of Technology,
ul. Krasińskiego 8, 40-019 Katowice, Poland
* Corresponding author: E-mail address: kazimierz.ducki@polsl.pl

Received 16.12.2007; published in revised form 01.02.2008

ABSTRACT

Purpose: The paper addresses the problem of determining the dependence between initial heat treatment of an austenitic Fe–Ni alloy and its mechanical properties and fatigue life at room temperature.

Design/methodology/approach: For the investigated Fe–Ni alloy after solution heat treatment, two variants of specimen ageing were applied for comparison, i.e. typical single-stage ageing and novel two-stage ageing. Specimens that underwent heat treatment were subjected to a static tensile test and low-cycle fatigue tests (LCF), carried out at room temperature.

Findings: It has been found that, the specimens of Fe–Ni alloy after two-stage ageing are distinguished by higher strength properties with a little lower plastic properties. In a case of low-cycle fatigue tests, specimens after single-stage ageing were characterized by higher fatigue life. Lower fatigue life of the alloy after two-stage ageing can be explained by increased brittleness of material in boundary areas.

Practical implications: The fatigue life results obtained in LCF conditions can be used in predicting the duration of operation of products made out of Fe–Ni alloy at room temperature.

Originality/value: The significance of the applied ageing variants' effect on the mechanical properties and fatigue life of the tested austenitic Fe–Ni alloy is shown in the paper.

Keywords: Fatigue; Metallic alloys; Heat treatment; Structure

PROPERTIES

1. Introduction

Austenitic Fe–Ni alloys precipitation-strengthened with intermetallic phases of type γ' [$Ni_3(Al,Ti)$] obtain their optimum properties after multi-stage heat treatment consisting of solution treatment (or annealing) and various ageing variants. Most frequently for such type of alloys, solution heat treatment from a temperature 980-1010°C and single-stage ageing at temperature of 710-730°C during 16-20h are applied [1-6]. For some Fe–Ni alloys after solution, it is recommended to apply two-stage ageing, which consists of carrying out a controlled cooling cycle between two isothermal soaking processes [7, 8].

In the presented paper, investigation was initiated concerning the effect of initial heat treatment on the fatigue life at room temperature of A-286 type high-temperature austenitic alloy. Specimens of Fe–Ni alloy were subject to tests after two variants of heat treatment, i.e. solution heat treatment followed by typical single-stage ageing, and solution heat treatment followed by novel two-stage ageing.

2. Material and procedure

The examinations were performed on rolled bars, 16 mm in diameter, of an austenitic Fe–Ni alloy. The chemical composition of the material is given in Table 1.

Table 1.
Chemical composition of the investigated Fe–Ni alloy.

Content of an element (wt.%)										
C	Si	Mn	Cr	Ni	Mo	V	Ti	Al	B	N
0.05	0.55	1.25	14.3	24.5	1.34	0.41	1.88	0.16	0.007	0.0062

Specimens of Fe–Ni alloy were subjected to tests after two variants of heat treatment, i.e. solution heat treatment and single-stage ageing (variant A) and solution heat treatment followed by two-stage ageing (variant B). Parameters of heat treatment for the investigated Fe–Ni alloy were determined based on the previously carried out studies [9-11] and data from professional literature [7, 8]. For the investigated alloy after solution heat treatment in the conditions: 980°C/2h/water, two variants of specimens' ageing were used for comparison, i.e.:

- single-stage ageing (variant A) : 715°C/16h/air;
- two-stage ageing (variant B) : 720°C/8h + cooling in the furnace up to a temperature of 650°C + 650°C/8h/air.

On heat-treated specimens according to variants A and B, static tensile test and low-cycle fatigue test were performed in the range $\Delta\varepsilon_t = 0.6\text{-}1.4$ % at room temperature.

A static tensile test at room temperature was carried out using a strength testing machine MTS-810. A yield strength (Y.S), tensile strength (T.S), unit elongation (EL.) and reduction of area (R.A) were determined.

Low-cycle fatigue tests were carried out at room temperature, using a servo-hydraulic system, MTS-810. The tests were carried with the servo-hydraulic machine being controlled by strain (the so-called fixed control) for the range of total strain $\Delta\varepsilon_t$ from 0.6 to 1.4 %. In a sinusoidal deformation cycle, an average strain rate $\dot{\varepsilon} = 2.0\times10^{-5}\ \mathrm{s}^{-1}$ was applied. The number of cycles until failure of specimen N_f was assumed to be the criterion of the investigated materials' durability [12-14].

Tests of the specimens' substructure after initial heat treatment were carried out using a thin foil technique on a Jeol transmission electron microscope, JEM-2000 FX, at accelerating voltage of 160 kV.

A Jeol JSM-35 scanning microscope was used for the observation of specimens' fractures. The aim of the observation was a fatigue analysis of the fractured specimens produced during the low-cycle fatigue tests.

3. Experimental results

The results of specimens' TEM observations of the Fe–Ni alloy after both variants of heat treatment demonstrated a diversified course of precipitation processes (Figs. 1, 2). It has been found that the precipitation process in the alloy substructure for variant A took place mainly within the matrix, where a characteristic "tweed-like" contrast connected with the occurrence of coherent precipitates of the intermetallic phase type γ' [$Ni_3(Al,Ti)$] and lenticular particles of phase G [$Ni_{16}Ti_6Si_7$] was identified (Fig. 1). As for variant B, the precipitation process of secondary phase particles took place both within the matrix and along the grain boundaries (Fig. 2). Early stages of type γ' phase precipitates were observed in the matrix, whereas within the area of grain boundaries, the occurrence of $M_{23}C_6$ carbide lamellae and lenticular particles of the G intermetallic phase were observed [10, 11].

Research results of the Fe–Ni alloy strength and plasticity related properties in its initial state, i.e. after solution heat treatment and 1-stage ageing (variant A) and after solution heat treatment and 2-stage ageing at room temperature are quoted in Table 2.

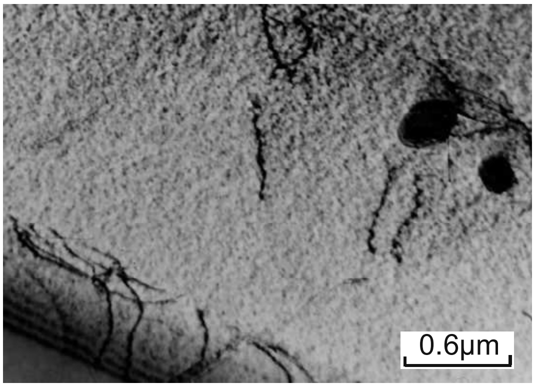

Fig. 1. Alloy substructure after heat treatment according to variant A. Coherent precipitates of phase γ' and lenticular particles of phase G in the matrix

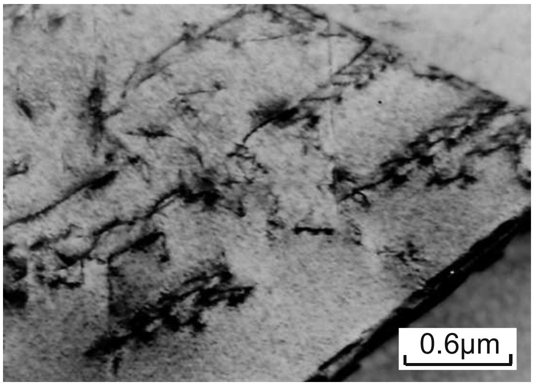

Fig. 2. Alloy substructure after heat treatment according to variant B. Coherent precipitates of phase γ' in the matrix and $M_{23}C_6$ carbide lamellae, and phase G particles on grain boundary

Table 2.
Mechanical properties of the Fe–Ni alloy after ageing according to variants A and B

Variant of ageing	Test temperature [°C]	Y.S [MPa]	T.S [MPa]	EL. [%]	R.A [%]
A	20	701	1021	27	48
B		761	1097	26	46

Based on the provided results it can be seen that the specimens subjected to 2-stage ageing (variant B) demonstrated better strength properties. Higher strength-related properties with the slightly lower plastic properties of the specimens after 2-stage ageing can be accounted for by stronger strengthening of grain boundaries and the zones near boundaries through precipitation of $M_{23}C_6$ carbides and phase G [$Ni_{16}Ti_6Si_7$] [10, 11].

The results of fatigue tests conducted at room temperature on Fe–Ni alloy specimens heat treated according to variants A and B are provided in Table 3 and presented in Figs. 3, 4. During the low-cycle fatigue tests for individual ranges of total strain $\Delta\varepsilon_t$ (0.6-1.4%), the values of amplitudal stress σ_a were determined depending on the number of cycles N. Based on those data, graphs of cyclic soaking were built and the values of saturation stress $\sigma_{\alpha n}$ were determined for the studied alloy.

Table 3.
Results of low-cycle fatigue tests of the Fe–Ni alloy specimens for variants A and B at a temperature of 20°C

Variant of ageing	Ranges of strain				σ_{an} [MPa]	N_f
	$\Delta\varepsilon_t$		$\Delta\varepsilon_e$	$\Delta\varepsilon_p$		
A	0.6%	0.006	0.0054	0.0006	593	23770
	0.8%	0.008	0.0060	0.0020	634	13520
	1.0%	0.010	0.0064	0.0036	677	9064
	1.2%	0.012	0.0068	0.0052	717	5820
	1.4%	0.014	0.0071	0.0069	744	3120
B	0.6%	0.006	0.0055	0.0005	611	20460
	0.8%	0.008	0.0064	0.0016	675	11740
	1.0%	0.010	0.0068	0.0032	712	6120
	1.2%	0.012	0.0072	0.0048	725	4320
	1.4%	0.014	0.0074	0066	737	2790

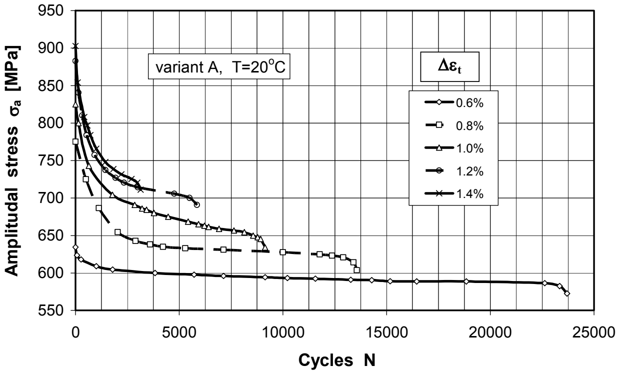

Fig. 3. Cyclic softening curves of the Fe–Ni alloy for variant A

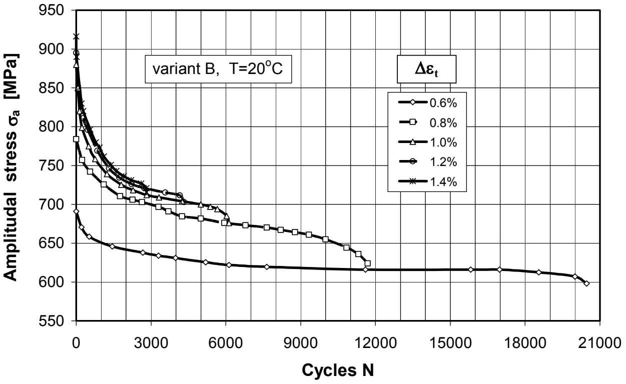

Fig. 4. Cyclic softening curves of the Fe–Ni alloy for variant B

As results from the low-cycle tests conducted at a temperature of 20°C, the specimens subjected to ageing according to variant A show higher fatigue durability. In both variants of heat treatment, the Fe–Ni alloy is characterized by cyclic softening in the low-cycle fatigue conditions.

The ranges of plastic strain $\Delta\varepsilon_p$ and elastic strain $\Delta\varepsilon_e$ and their corresponding stress range $\Delta\sigma$, were determined on the basis of a hysteresis loop recorded in the course of the testing. The fatigue durability values for the Fe–Ni alloy at room temperature were described by the Smith, Hirschberg and Manson dependence [15]:

$$\Delta\varepsilon_t = \Delta\varepsilon_p + \Delta\varepsilon_e = M \cdot N_f^z + (G / E) \cdot N_f^\nu \quad (1)$$

where: M, G, E, z, ν – material constants.

The results of the Fe–Ni alloy fatigue durability at room temperature are provided in Table 4.

Table 4.
Mathematical models of the Fe–Ni alloy specimens' fatigue durability for variant A and B at room temperature

Variant of ageing	$\Delta\varepsilon_p = M \cdot N_f^z$		$\Delta\varepsilon_e = (G/E) \cdot N_f^\nu$	
	M	z	G/E	ν
A	126.0	–1.18	0.0217	–0.136
B	188.4	–1.27	0.0240	–0.144

Having obtained the saturation stress values σ_{an} for amplitudal plastic strain ε_p, mathematical models (2) of cyclic alloy deformation were devised, as presented in Table 5. Also, a cyclic strength coefficient (K') and a cyclic softening exponent (n') were determined for the studied alloy [15]:

$$\sigma_{an} = K' \cdot (\Delta\varepsilon_p / 2)^{n'} \quad (2)$$

where: K' – cyclic strength coefficient, n' – cyclic softening exponent.

Table 5.
Values of coefficient (K') and exponents (n') for the Fe–Ni alloy deformation curves at 20°C of variants A and B

Variant of ageing	ε_p	σ_{an} [MPa]	K' [MPa]	n'
A	0.0003	593	1233.2	0.092
	0.0010	634		
	0.0018	677		
	0.0026	717		
	0.0034	744		
B	0.0025	611	1131.7	0.074
	0.0008	675		
	0.0016	712		
	0.0024	725		
	0.0033	737		

Fractographic observations were conducted on the Fe–Ni specimen fractures after low-cycle fatigue at room temperature. After low-cycle fatigue tests conducted until total strain $\Delta\varepsilon_t$ = 0.8%, the specimens demonstrated a certain diversification in terms of the obtained fractures' morphology (Figs. 5, 6). In variant A specimens, a typical fatigue fracture with characteristic fatigue stripes and traces of significant plastic deformation were observed (Fig. 5). In the case of variant B specimens, the fatigue fracture was of a cleavage type, with a fraction of intergranular cracks and traces of slight plastic strain (Fig. 6).

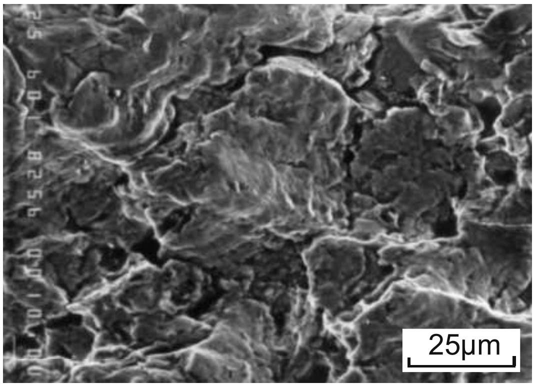

Fig. 5. Variant A specimen fatigue fracture after fatigue tests ($\Delta\varepsilon_t$=0.8%) at 20°C. Transcrystalline ductile fracture

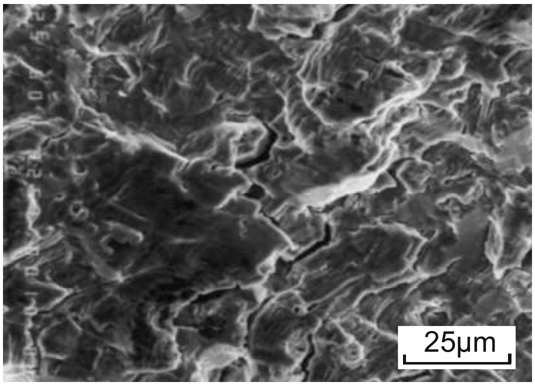

Fig. 6. Variant B specimen fatigue fracture after fatigue tests ($\Delta\varepsilon_t$=0.8%) at 20°C. Mixed transcrystalline fracture

4. Conclusions

The paper analyses the influence of initial heat treatment on the mechanical properties and structure of the austenitic Fe–Ni alloy precipitation-strengthened with intermetallic phases of the γ' [$Ni_3(Al,Ti)$] type. Specimens of the studied alloy after solution heat treatment were subjected to two ageing variants, i.e. 1-stage ageing at 715°C (variant A) and 2-stage ageing at 720°C and 650°C (variant B). On heat-treated specimens according to variants A and B, static tensile test and low-cycle fatigue test were performed in the range $\Delta\varepsilon_t$= 0.6-1.4 % at room temperature.

Static tensile tests conducted at a temperature of 20°C demonstrated higher strength properties of the specimens for variant B (Y.S = 761 MPa, T.S = 1097 MPa) compared to variant A (Y.S = 701 MPa, T.S = 1021 MPa), with their plastic properties being comparable.

The low-cycle fatigue tests proved a significant influence of the applied ageing variants A and B on the Fe–Ni alloy's fatigue durability at room temperature. The alloy's fatigue durability after heat treatment according to variant A was higher than the durability of the alloy heat treated according to variant B.

The reason for lower fatigue durability at room temperature of the heat treated specimens in variant B should be sought in a larger number of secondary phase particles precipitated on grain boundaries, which determines earlier initiation of the fatigue cracking process.

References

[1] M. Konter, M. Thumann, Materials and manufacturing of advanced industrial gas turbine components, Journal of Materials Processing Technology 117 (2001) 386-390.

[2] R. Shargi-Moshtaghin, S. Asgari, The influence of thermal exposure on the γ' precipitates characteristics and tensile of superalloy IN-738LC, Journal of Materials Processing Technology 147 (2004) 343-350.

[3] S.A. Sajjadi, S.M. Zebarjad, Effect of temperature on tensile fracture mechanisms of a Ni-base superalloy, Archives of Materials Science and Engineering 28/1 (2007) 34-40.

[4] S.A. Sajjadi, S.M. Zebarjad, Study of fracture mechanisms of a Ni-Base superalloy at different temperatures, Journal of Achievements in Materials and Manufacturing Engineering 18 (2006) 227-230.

[5] P. Jonsta, Z. Jonsta, J. Sojka, L. Cizek, A. Hernas, Structural characteristics of nickel superalloy Inconel 713LC after heat treatment, Journal of Achievements in Materials and Manufacturing Engineering 21/2 (2007) 29-32.

[6] N.S. Stoloff, Wrought and P/M superalloys, ASM Handbook, Vol. 1: Properties and Selection Irons, Steels and High-Performance Alloys, ASM Materials Information Society, 1990, 950-977.

[7] F. Schubert, Temperature and Time Dependent Transformation: Application to Heat Treatment of High Temperature Alloys, In: Phase Stability in High Temperature Alloys, Appied Science Publishers , London, 1981, 119-149.

[8] Ch.T. Sims, N.S. Stoloff, W.C. Hagel, Superalloys II, Ed. A. Wiley Witescience Publications, 1987, New York.

[9] K.J. Ducki, M. Hetmańczyk, The influence of prolonged aging on the structure and properties of precipitation hardened austenitic alloy, Materials Engineering, Sigma NOT, Warsaw 4 (2001) 290-293.

[10] K.J. Ducki, Analysis of the precipitation and growth processes of intermetallic phase in a high-temperature Fe–Ni alloy, Materials Engineering, Sigma NOT, Warsaw 2 (2007) 53-58 (in Polish).

[11] K.J. Ducki, Structure and precipitation strengthening in a high-temperature Fe–Ni alloy, Archives of Materials Science and Engineering 28/4 (2007) 203-210.

[12] J. Okrajni, M. Cieśla, L. Swadźba, High-temperature low-cycle fatigue and creep behaviour of nickel-based superalloys with heat-resistant coating, Fatigue and Fracture of Materials and Engineering Structures 21 (1998) 947-954.

[13] Z. Gronostajski, K. Jaśkiewicz, Influence of monotonic and cyclic deformation sequence on behaviour of CuSi3.5 silicon bronze, Journal of Achievements in Materials and Manufacturing Engineering 15 (2006) 39-46.

[14] J. Okrajni, A. Marek, G. Junak, Description of the deformation process under thermo-mechanical fatigue, Journal of Achievements in Materials and Manufacturing Engineering 21/2 (2007) 15-23.

[15] S. Kocańda, A fatigue cracking of metals, WNT, Warsaw, 1985 (in Polish).